Welding in the World (2024) 68:1485–1495
https://doi.org/10.1007/s40194-024-01719-3

RESEARCH PAPER

Control of meltpool shape in laser welding

Wojciech Suder[1] · Xin Chen[1] · David Rico Sierra[1] · Guangyu Chen[1] · James Wainwright[1] · Kuladeep Rajamudili[1] · Goncalo Rodrigues Pardal[1] · Stewart Williams[1]

Received: 18 August 2023 / Accepted: 8 February 2024 / Published online: 5 March 2024
© The Author(s) 2024

Abstract
In laser welding, the achievement of high productivity and precision is a relatively easy task; however, it is not always obvious how to achieve sound welds without defects. The localised laser energy promotes narrow meltpools with steep thermal gradients, additionally agitated by the vapour plume, which can potentially lead to many instabilities and defects. In the past years, there have been many techniques demonstrated on how to improve the quality and tolerance of laser welding, such as wobble welding or hybrid processes, but to utilise the full potential of lasers, we need to understand how to tailor the laser energy to meet the process and material requirements. Understanding and controlling the melt flow is one of the most important aspects in laser welding. In this work, the outcome of an extensive research programme focused on the understanding of meltpool dynamics and control of bead shape in laser welding is discussed. The results of instrumented experimentation, supported by computational fluid dynamic modelling, give insight into the fundamental aspects of meltpool formation, flow direction, feedstock melting and the likelihood of defect formation in the material upon laser interaction. The work contributes to a better understanding of the existing processes, as well as the development of a new range of process regimes with higher process stability, improved efficiency and higher productivity than standard laser welding. Several examples including ultra-stable keyhole welding and wobble welding and a highly efficient laser wire melting are demonstrated. In addition, the authors present a new welding process, derived from a new concept of the meltpool flow and shape control by dynamic beam shaping. The new process has proven to have many potential advantages in welding, cladding and repair applications.

Keywords Laser welding · Meltpool control · Melt flow · Dynamic beam shaping

1 Introduction

Prevention of defects and control of weld quality is one of the biggest challenges in high-productivity power beam welding processes, such as laser welding. A typical meltpool in laser welding is subject to many competing forces, which can be difficult to balance [1]. The highly focused laser energy can easily lead to a steep temperature gradient, which then induces rapid convective flow in order to equalise the temperature in the liquid metal [2]. Several studies showed the underlying mechanisms of different components contributing to the net flow in laser welding, such as Marangoni convection, buoyancy flow, flow due to friction of vapour gases and capillary flow due to the welding speed [3]. All these components have a major influence on the final weld, and depending on the viscosity of the material and processing conditions (laser power, travel speed and spot size), a variety of different regimes can be achieved. This means that sometimes altering one of the processing parameters can lead to a remarkable difference in the weld profile or likelihood of defect formation. Furthermore, unlike in most low productivity processes, in laser welding, the timescales for defect formation and the solidification time are very short making an in situ defect detection more challenging [4, 5].

In most scenarios, the Marangoni convection is one of the dominant forces in the liquid metal flow and its direction usually follows the temperature gradient. This opens a window for control of this flow and the improvement of various aspects of weld quality. Modification of the laser profile or beam shaping is one of the most common approaches to flexible control of the energy distribution

Recommended for publication by Commission IV - Power Beam Processes.

✉ Wojciech Suder
w.j.suder@cranfield.ac.uk

[1] Welding and Additive Manufacturing Centre, Cranfield University, Cranfield MK43 0AL, UK

of a laser beam and hence the temperature gradient. Several different techniques of beam shaping are possible but the most common and industrially viable use diffractive optics [6, 7], refractive optics [8, 9] or spatial manipulation of fibre delivery optics [10, 11]. In all cases, a precisely engineered manipulation of the optical path redistributes the incoming laser beam and modifies its energy distribution in the workpiece. Positive effects on the microstructural development, bead quality improvement and melt flow modification have been demonstrated [10, 12, 13]. In addition, a cyclic oscillation of a circular laser spot by galvo-scanning optics, referred to as wobble welding, gained attention in the last years. This method allows for an effective control of the temperature gradient and melt flow [14]. Several benefits on the weld profile and process stability have been reported to be achieved with this technique, mostly in micro-welding applications [15–17]. Many publications focus on technical aspects of beam shaping or its influence on the final weld; however, there is no general understanding of their effect on the meltpool dynamics and overall process stability. In other means, when it comes to practical aspects of laser welding, it is unclear how to set up the process in order to operate it in the most stable conditions with well-balanced forces within the meltpool.

In this paper, we report the results of an ongoing research programme focused on the understanding of the phenomena responsible for weld bead formation and feedstock melting in laser welding and additive manufacturing. Various cases from numerical modelling and experimental validations are shown. Two new welding regimes are proposed, and the work draws some useful recommendations for laser users. The main aim of the paper is to demonstrate, based on a few case studies, how with the aid of CFD modelling we can control and maximise the stability of the meltpool in laser processing.

2 Methods

To understand the flow behaviour in different processing regimes, numerical modelling and various experiments were carried out. The experiments were carried out on four different set-ups, as summarised in Table 1. Each was optimised for a specific process, such as conduction welding, laser wire melting, keyhole laser welding, wobble welding and some new regimes. In all cases, two different camera systems were used to observe the meltpool, a compact welding camera (Xiris XVC1000) for generic observations and a high-speed camera (HSVC NAC/Phantom 710S) with a laser illumination (Oxford Lasers FireBIRD 1000w) for detailed studies of the melt flow, as shown in Fig. 4. In addition, in some cases, tungsten carbide particles were added to the liquid metal to trace the flow pattern. In all cases, pure shield argon was used.

2.1 Keyhole/conduction—conventional laser welding regimes

Conduction, keyhole and wire melting experiments were carried out on an 8-kW (IPG Photonics) fibre laser interfaced with a Fanuc robotic manipulator and a Dinse wire feeder, as shown in Fig. 1. Depending on the size of the meltpool, either a side nozzle or a trailing shoe was used for shielding, both supplied with pure shield argon. Two different materials were used, 12-mm S355 steel plates for keyhole and conduction welds and 10-mm Ti_6Al_4V plates with a 1.2-mm Ti_6Al_4V wire for laser wire experiments.

2.2 Wobble welding

Wobble laser welding experiments were carried out on a 500-W single-mode (SPI Lasers) fibre laser coupled with a Raylase galvo-scanner equipped with a 400-mm lens, as shown in Fig. 2. Pure shield argon was supplied through a ceramic nozzle to provide shielding from ambient air. All

Table 1 Laser systems used in this research

Item	Laser type	Laser max. power	Fibre diameter	Optics type	Spot size used	Figure showing set-up
Keyhole/conduction welding and laser wire	Fibre, multimode	8 kW	300 µm	Fixed head	600 µm	Figure 1
Wobble welding	Fibre, single-mode	2 kW	20 µm	Galvo-scanner	100 µm	Figure 2
Concentric twin spot	2 × fibre lasers arranged spatially	8 kW 3 kW	300 µm 50 µm	2 × fixed laser heads	10–15 mm 100 µm	Figure 3
Multi-energy source	Fibre multimode + plasma transferred arc	6 kW 450 A (plasma)	100 µm	Galvo-scanner + arc source	4 mm	Figure 4

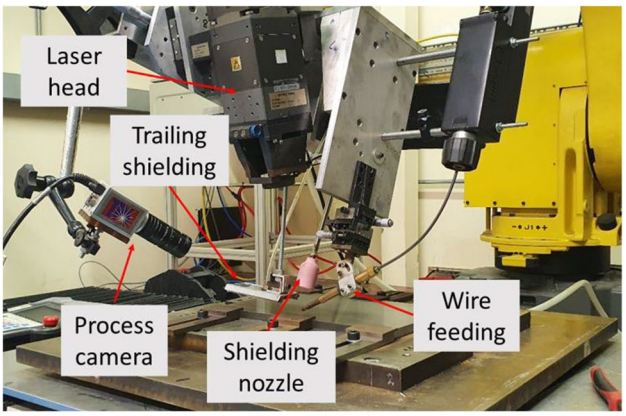

Fig. 1 Experimental set-up for conventional laser regimes, 8-kW multimode laser, robotic manipulator and wire feeder

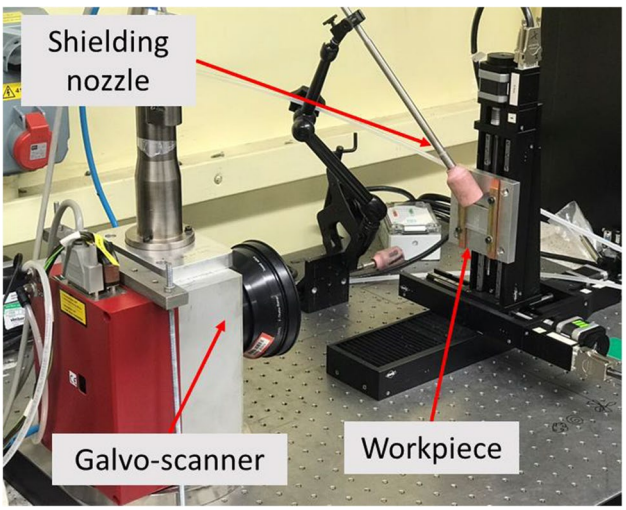

Fig. 2 Experimental set-up for wobble welding, 500-W single-mode laser with galvo-scanner with 400-mm objective

wobble welds were carried out in 2-mm-thick 1xxx series aluminium plates.

2.3 Concentric twin spot welding

After understanding the main requirements for stable keyhole welding, a new improved keyhole regime was investigated, referred to as concentric twin spot welding. The experiments required a complex energy distribution profile, which was achieved with two separate lasers, a 3-kW fibre laser (SPI Lasers) with 100-µm spot size and an 8-kW fibre laser (IPG Photonics) defocused to 10- to 15-mm spot size. Both laser heads were mounted onto a Fanuc robotic manipulator, as shown in Fig. 3. The first beam generated a keyhole regime with deep penetration, whilst the second beam generated a conduction regime with a large meltpool around the keyhole. The liquid metal was protected by a specially designed trailing shielding nozzle supplied with pure shield argon. The material welded was S355 steel with a thickness of 10 mm.

2.4 Multi-energy source MES process

A new laser wire melting process was investigated, which required the integration of a 6-kW fibre laser delivered by means of a high-power galvo-scanner (IPG Photonics) and a plasma transfer arc source (EWM) with a wire feeder (Dinse). The laser was interfaced with a 5-axis gantry motion system (Aerotech), as shown in Fig. 4. The galvo-scanner was used for beam shaping. The laser spot was being oscillated in a linear pattern at a relatively high speed to redistribute the laser energy and form a relatively wide weld bead. Two different cases were used, a constant energy profile and a variable energy profile, as shown in Fig. 5. In the first case, the programmed oscillation speed for each line was constant, set

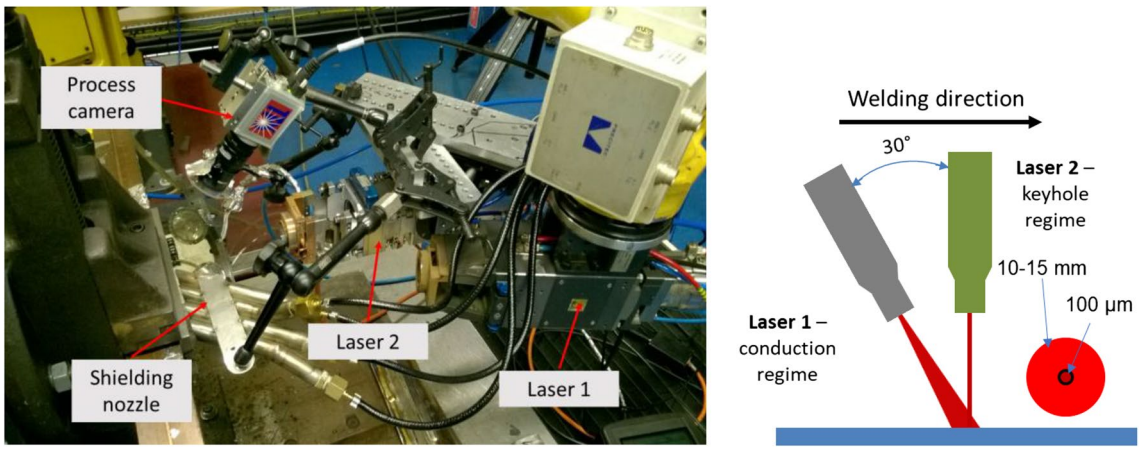

Fig. 3 Experimental set-up for superimposed keyhole-conduction regime, 8-kW and 3-kW multimode lasers arranged in a concentric configuration

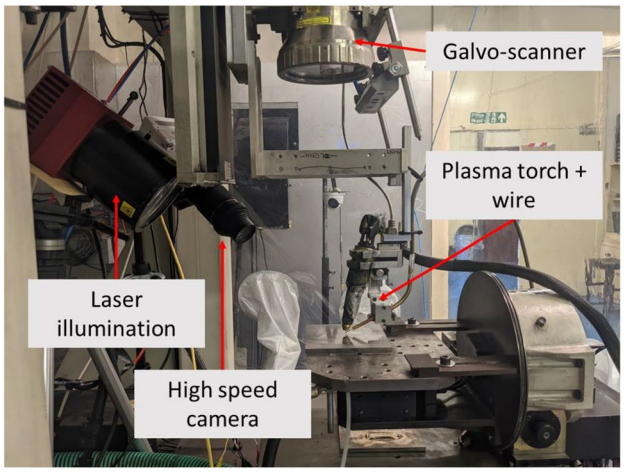

Fig. 4 Experimental set-up used for multi-energy source experiments, 6-kW multimode laser, 400A plasma source and a wire feeder

at 200 mm/s at all times. In the variable energy case, the oscillation speed was set to 200 mm/s only for the first 4 mm of the scanning amplitude, followed by a rapid rise of scanning speed, the maximum allowed speed of the scanner and then a gradual increase back to 200 mm/s in the last 4 mm of the scanning amplitude. This allowed us to change the transient energy and hence energy density over the programmed pattern. The laser spot size and amplitude of oscillation were 4 mm and 20 mm respectively. The average oscillation speed was adjusted to achieve different energy profiles. In this case, due to the complexity of the set-up, the whole system was enclosed in a flexible argon enclosure filled with pure shield argon. Ten-millimetre Ti_6Al_4V plates and a 1.2-mm Ti_6Al_4V wire were used as the substrate and feedstock material.

2.5 Fluid flow modelling

Numerical simulations of different laser welding processing regimes, such as laser conduction welding, wire feed laser welding, keyhole welding, wobble laser welding and new hybrid welding, have been conducted to investigate the dynamics of the fluid flow behaviour. In the simulations, the liquid metal was assumed as a laminar, Newtonian, incompressible fluid, following previously reported modelling work [18–21]. The volume of fluid (VOF) [22] or TruVOF [23] method and enthalpy-porosity technique [24] were used to track the time-dependent liquid–gas interface (free surface) and solid–liquid interface, respectively. The wire movement in the simulation of the wire feed welding process was described by using a mixture theory and Euler method [25, 26]. The incompressible thermal fluid flow was described by the three conservation equations of mass, momentum and energy:

$$\nabla \cdot u = 0, \tag{1}$$

$$\rho\left(\frac{\partial \mathrm{u}}{\partial t} + (u \cdot \nabla)u\right) = -\nabla p + \nabla \cdot (\mu \nabla u) + F_{\mathrm{b}} + F_{\mathrm{s}}, \tag{2}$$

$$\rho\left(\frac{\partial h}{\partial t} + (u \cdot \nabla)h\right) = \nabla \cdot (k \nabla T) + q_{\mathrm{heat}} + q_{\mathrm{loss}}, \tag{3}$$

where ∇ is the Hamiltonian, u is the velocity vector, ρ is the density, t is the time, p is the pressure, μ is the dynamic

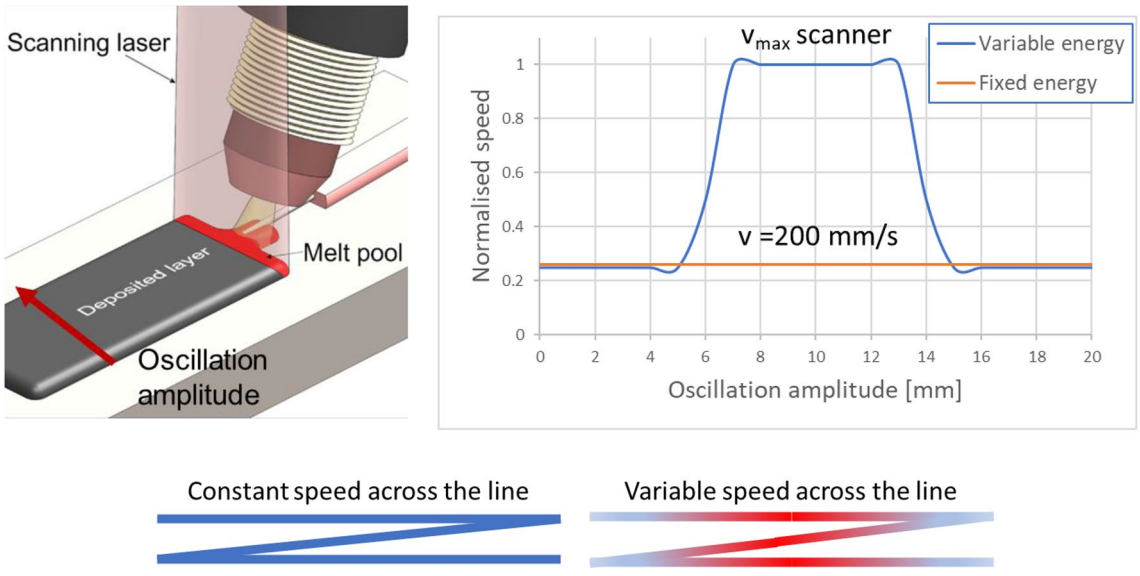

Fig. 5 Multi-energy source process with scanning laser and plasma transferred arc, two different energy distributions, variable and fixed energy across the weld bead width achieved by different beam scanning techniques

viscosity, h is the enthalpy, and k is the heat conductivity. F_b is the body force, including gravity, buoyancy, Darcy force and electromagnetic force. F_s is the surface force, including surface tension, Marangoni shear stress, recoil pressure, arc pressure and arc shear stress. q_{heat} is the heat source. q_{loss} is the heat loss caused by gas convection, thermal radiation and possible evaporation.

Moreover, in all the simulations except for the wobble laser welding process, a commercial CFD solver Ansys-Fluent 2019R2 was used to solve the governing equations and VOF equation. A non-uniform hexahedral mesh with a size of 0.1–1 mm was used to balance the accuracy and efficiency of the simulations. A time step with a value between 2.5×10^{-5} and 5×10^{-5} s was used to obtain a robust convergence. For the simulations of the wobble laser welding process, a Flow-3D v12.0 solver was used to solve the governing equations and TruVOF equation. A uniform hexahedral mesh with a size of 0.025 mm and a time step of 1.0×10^{-6} s was used for good accuracy and robust convergence. Full details of the models, boundary conditions and thermophysical properties used in the simulations can be found in other publications [1, 25, 27]. The process parameters used in the simulations were the same as those used in the experiments.

3 Results and discussion

One of the main advantages of lasers is the ability to operate in a variety of regimes and processing conditions. The meltpool development and its stability are one of the primary challenges in laser welding, and can influence the bead profile, defect formation and microstructural development. Some regimes are rather simple with only a few variables to control and only one or two major forces acting on the meltpool. An example of such a regime is conduction welding with the surface tension gradient, referred to as Marangoni convection as the main driving force for the melt flow. In contrast, keyhole or wobble welding requires control of several variables and many driving forces can influence the flow of the liquid metal. Normally, the fewer the components contributing to the net flow, the easier it is to predict and control it. Hence, it is important to understand different regimes separately.

3.1 Surface tension regime

In the absence of vaporisation, when the energy density of the laser beam is below the vaporisation threshold for a given material, the meltpool tends to acquire a symmetric shape with a hemispherical fusion boundary, as shown in Fig. 6. The flow velocity vectors follow the temperature gradient, but their magnitude is low. The fusion boundary is slightly asymmetric, due to the additional influence of the welding speed. However, generally, this regime does not experience any complex flow pattern and its direction and magnitude are mostly entirely dependent on the temperature gradient. Hence, in conduction welding, the intensity distribution profile of the laser spot has a major influence on the flow pattern, and hence, beam shaping is one the most effective ways of controlling it.

The situation is slightly more complex with the addition of a feedstock wire. Most liquid metals require significant effort to overcome the cohesive force between the molecules as the system tries to minimise its surface energy. Therefore, any interruption of the meltpool by an external object normally results in altering its shape and flow pattern. In Fig. 7, an example of melt flow behaviour in the conduction regime with the additional filler wire is shown. When the droplet is not in contact with the main meltpool, the forces are quite balanced without any dominant direction of the flow. However, as soon as the droplet makes the contact with the meltpool, we can observe a sudden change in its shape and alteration of the flow direction. The droplet and the main meltpool become slightly elongated, and the meltpool becomes shallower due to the drag force of the cohesive forces. In addition, the velocity vectors develop directionality, indicating a weak flow towards the wire. As soon as the droplet detaches from the wire tip, the meltpool tries to relax to its steady-state shape driven by the surface tension force.

The meltpool experiences periodic interruptions every time the droplet is detached, followed by its relaxation to its nominal shape, before being interrupted again. Note that in the case presented in Fig. 7, the droplet detachment interval was approximately 0.8 s. Hence, the duration between two subsequent droplet detachment events was not sufficient for the meltpool to achieve a fully nominal shape. The fact that a perfectly stable meltpool can be interrupted by the contact with an external object, such as a feedstock wire or a droplet,

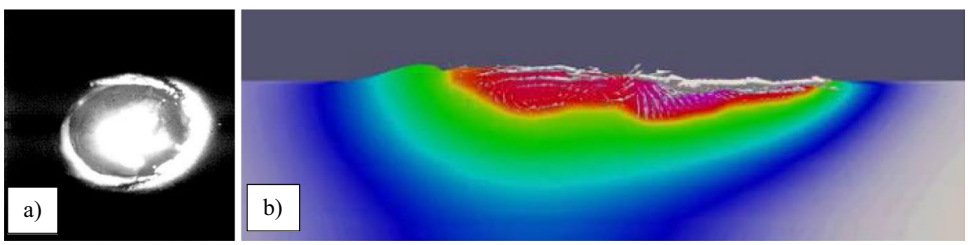

Fig. 6 Conduction weld in S355 steel, laser power 8 kW, travel speed 0.3 m/min, laser spot size 12 mm; **a** top view of meltpool, **b** modelling results of fusion boundary in the longitudinal direction

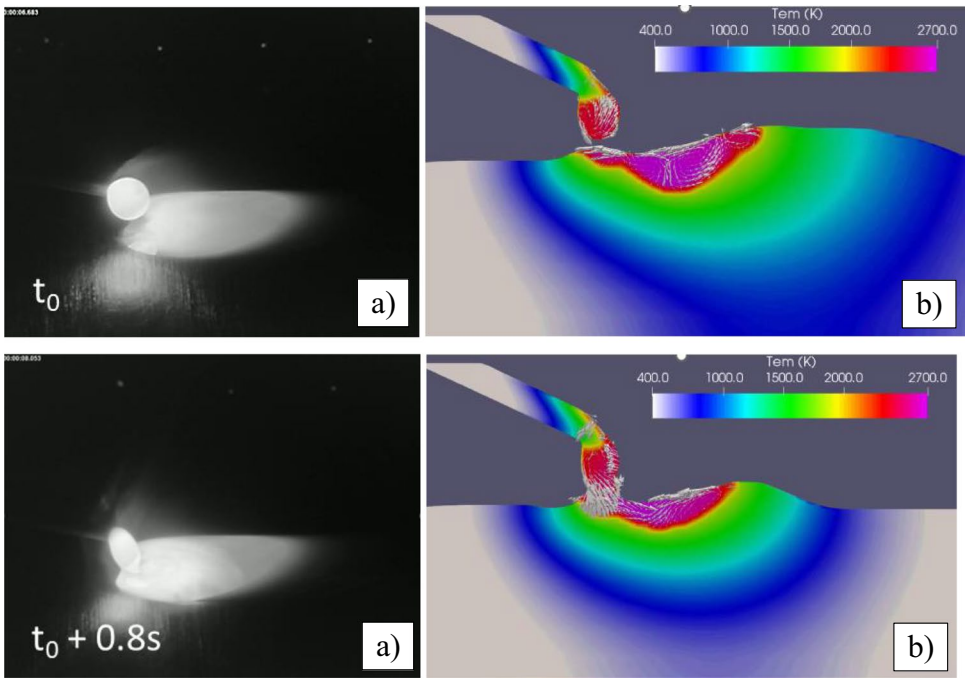

Fig. 7 Laser wire melting of Ti_6Al_4V, laser power 4 kW, travel speed 0.3 m/min, laser spot size 8 mm, wire feed speed 2 m/min; **a** top view of meltpool, **b** modelling results of fusion boundary in the longitudinal direction

indicates that the strength of the temperature gradient-driven flow in liquid metals is relatively low.

3.2 Drag enhanced regime

In keyhole laser welding, apart from the Marangoni convection, other forces, such as recoil pressure, friction of escaping gases and capillary force, are amongst other dominant forces inducing the motion of the liquid metal. At low welding speeds, the recoil force of the vapour pressure is dominant resulting in a downward flow of the liquid metal, as shown in Fig. 8. This can lead to the accumulation of heat at the bottom of the keyhole, which then tends to induce a strong circular flow driven by Marangoni convection, trying to balance the temperature distribution. The downward flow is known to be undesirable due to the high risk of gas entrapment and other defects [28]. Also, this kind of system with a deep and narrow keyhole does not allow for efficient ejection of vapour gases and is likely to generate spatter.

An increase in welding speed is known to cause inclination of the keyhole and a simultaneous change in the flow direction. The escaping gases from the bottom of the keyhole induce a shear force onto the rear wall of the keyhole, resulting in enlarging its exit diameter, as shown in Fig. 9. On the one hand, this upward flow and increased keyhole diameter have a positive effect on porosity mitigation and keyhole stability. On the other hand, the flow pattern can be quite dynamic, resulting in strong vortexes and spatter. This is an example of drag force enhanced melt flow, which counteracts the Marangoni convective flow.

A similar principle of elongated keyhole is used in wobble welding. In this regime, a relatively small keyhole is rapidly moved in a periodic pattern to mechanically spread the meltpool and avoid localised overheating of the material. An example of a fusion zone achieved with dynamically spread energy is shown in Fig. 10. The modelling result and experimental validations are in good agreement. If the laser beam is oscillated fast enough, faster than the characteristic time needed for solidification, then a wide homogenous

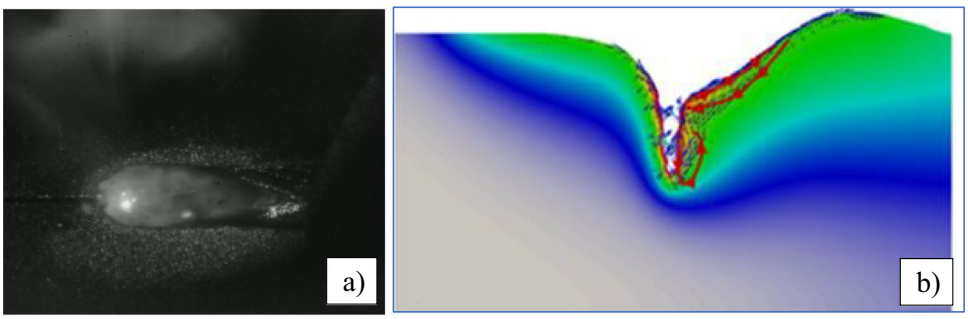

Fig. 8 Keyhole laser welding in S355 steel, laser power 8 kW, travel speed 1 m/min, laser spot size 0.6 mm; **a** top view of meltpool, **b** modelling results of fusion boundary in longitudinal direction

meltpool is generated. This mechanical oscillation not only affects the spread of the liquid metal but also allows for control of the liquid flow direction. In certain cases, the melt flow due to Marangoni convection is completely suppressed and a new flow of the drag force due to the motion of the beam becomes dominant. The flow direction, its magnitude and the meltpool stability are dependent on the beam motion parameters.

As shown in Fig. 11a, at optimum conditions, the keyhole is stable despite a significantly bigger meltpool size to keyhole size ratio. The keyhole is well balanced, and both the convective flow and keyhole natural perturbations are mostly suppressed. The right combination of angular velocity and size of the meltpool resulted in a slightly elongated keyhole with a highly stable meltpool. Note that the angular velocity in this case was controlled indirectly by the oscillation frequency and amplitude. Increasing the power (Fig. 11b) or frequency (Fig. 11c) resulted in either too large meltpool or too high angular velocity and led to destabilisation of the system. A further increase of laser power resulted in excessive accumulation of energy, which could not be redistributed fast enough even at higher oscillation frequency (angular velocity) and led to instabilities. At higher frequency (Fig. 11c), the beam motion induced excessive drag on the meltpool and accelerated the liquid metal beyond the stable limit for the surface tension forces to balance it, which led to melt expulsion, spatter and dynamic instabilities. This indicates that to successfully apply the dynamic control of the keyhole and meltpool, the right velocity needs to be applied for given material's viscosity, density and thermal properties.

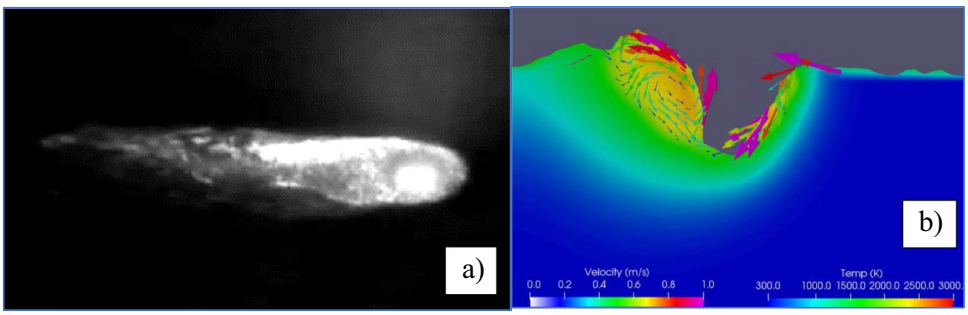

Fig. 9 Keyhole laser welding in S355 steel, laser power 8 kW, travel speed 4 m/min, laser spot size 0.6 mm; **a** top view of meltpool, **b** modelling results of fusion boundary in longitudinal direction

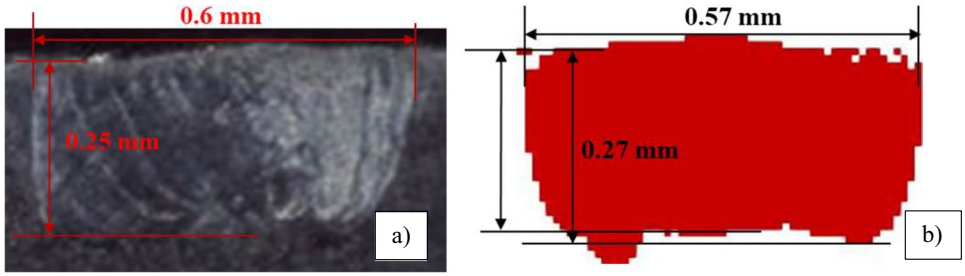

Fig. 10 Comparison of bead cross section between **a** experiment and **b** simulation in laser wobble welding of 1xxx series aluminium, travel speed 1.5 m/min, circular oscillation pattern, oscillation amplitude 0.2 mm, frequency 200 Hz and laser spot size 0.045 mm

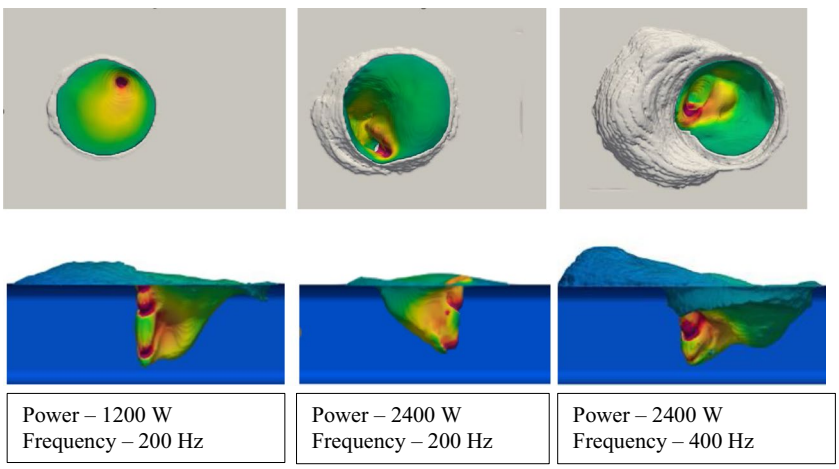

Fig. 11 Effect of oscillation frequency and laser power on the stability of keyhole in laser wobble welding of 1xxx series aluminium, travel speed 1.5 m/min, circular oscillation pattern, oscillation amplitude 0.7 mm and laser spot size 0.1 mm

3.3 Balanced drag enhanced regime

As demonstrated in the previous section, the keyhole regime can be difficult to get it right. At slow speeds and high powers, the large meltpool surrounding the keyhole can lead to necking and temporary keyhole collapse, which increases the likelihood of keyhole defects. The drag force of escaping vapour gases from inclined keyhole at high speeds, stabilises the keyhole, but also often leads to melt expulsion and spatter. A stable keyhole requires an optimum exit diameter, which should allow for efficient removal of gases but also it needs to maintain high pressure to enable deep penetration. A stable meltpool requires a temperature gradient to be kept to a minimum. Usually, it is challenging to optimise both of these important aspects of keyhole and meltpool stability with standard Gaussian or top hat energy profile beams. A small spot size, on the one hand, promotes the stability of the keyhole by minimising size of the meltpool, but the small keyhole and high-temperature gradient induce strong melt flow. A big spot size, on the other hand, leads to a larger keyhole size with better vapour gas removal ability but the larger meltpool can lead to keyhole collapse.

It is possible to achieve a well-balanced keyhole with a stable meltpool by the application of an advanced control of the intensity of a laser beam. In an example in Fig. 12, a complex beam profile with a high-intensity central section and a low-intensity but high-average energy outer section was applied. The high-intensity central section generated a deep and narrow keyhole, whilst the low-intensity high-power section provided an unagitated meltpool with low temperature gradient. It can be seen in Fig. 12 that the keyhole is stable, and the liquid metal does not tend to close it. The resulting weld profile ensures deep penetration and good quality. Another benefit of a bead profile with a small root size and a wide top bead is its excellent resilience to overpenetration and root sagging. Note that, in this particular case, this complex beam profile was achieved with two separate laser heads, but a similar effect can be potentially achieved with beam shaping. In Fig. 13, another example with an even larger low-intensity section is shown. The process exhibited an excellent stability, and the resulting weld profile shows an interesting alternative to normal keyhole welds.

3.4 Non-surface tension wire melting regime

Traditionally, in most laser wire melting applications, the laser is operated in a conduction regime, where a large laser spot generates the meltpool, into which the feedstock wire is immersed. The small meltpool in keyhole regimes requires high precision in pointing the wire and is less common than in the conduction regime. However, due to the unidirectional character of the heat conduction in metals, it is impossible to decouple the bead width from the depth of penetration, i.e. to achieve wide meltpools with low dilution or the other way around. In other words, conduction welds are highly

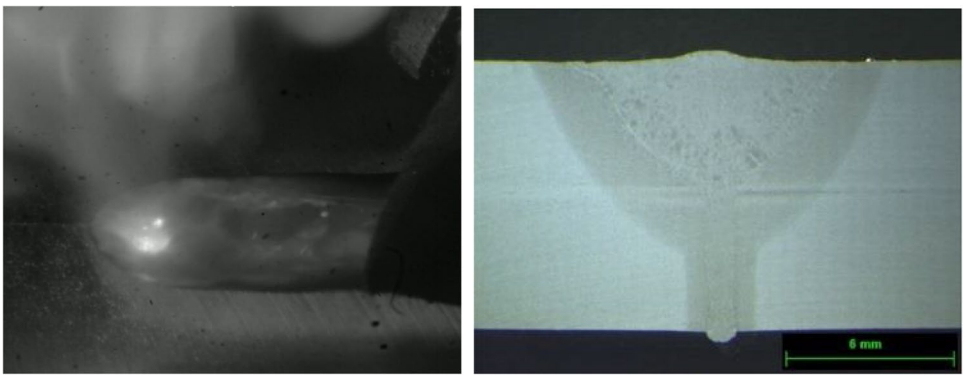

Fig. 12 Balanced keyhole by concentric twin spot welding at a welding speed of 0.5 m/min, keyhole laser (laser power 3 kW and spot size 0.1 mm) and conduction laser (laser power 8 kW and spot size 10 mm)

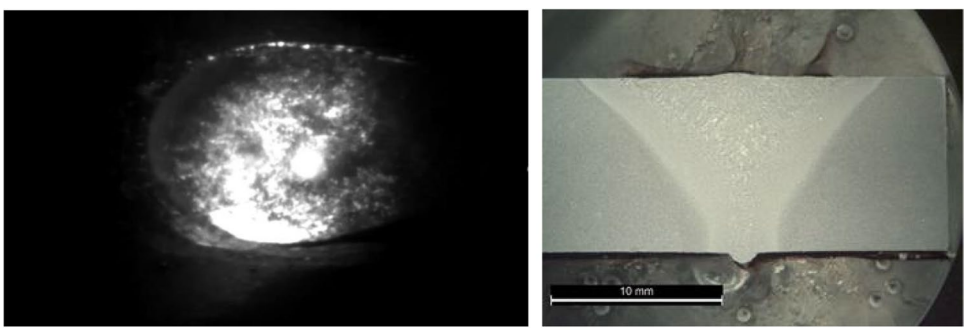

Fig. 13 Balanced keyhole by concentric twin spot welding at a welding speed of 0.5 m/min, keyhole laser (laser power 3 kW and spot size 0.1 mm) and conduction laser (laser power 8 kW and spot size 15 mm)

susceptible to three-dimensional heat flow. However, it is possible to decouple the heat conduction from convective flow with the application of a beam shaping and dynamic oscillation. In Fig. 14, an example of beam shaping with the use of galvo-scanner, referred to as dynamic beam shaping, is shown [29]. The combination of a multi-energy source (MES), consisting of an arc source and a laser beam oscillated by a galvo-scanner resulted in a complex energy profile (Fig. 14) in the workpiece and a fully controlled melt flow pattern. Evenly distributed energy resulted in a low temperature gradient and hence negligible Marangoni convection. The resulting top beads and cross sections are shown in Fig. 15. Since the flow in the meltpool is almost entirely controlled by the dynamic beam shaping, it was possible to tailor it and achieve different bead profiles. When applying a simple oscillation strategy with constant speed of oscillation, a weld-like bead shape with a convex reinforcement was achieved (Fig. 15a). Also, a typical shape of the solidification line, elongated towards the opposite direction to the welding direction, can be seen. This suggests that this process was able to control the weld width, but not to affect the melt flow significantly.

However, when applying a more sophisticated oscillation strategy with variable speed of oscillation, the temperature gradient could be controlled in a better extent, resulting not only in a flatter top bead, but also the shape of the solidification line is completely different, suggesting a non-standard meltpool shape prior to the solidification (Fig. 15b). This bead exhibits much flatter reinforcement and the solidification pattern is narrow in the longitudinal direction, which is not normal for such a large meltpool. This indicates that the flow magnitude in the longitudinal direction was low, which is consistent with the modelling data from Fig. 14c. The lack of strong longitudinal flow meant that the liquid metal could be more easily controlled and transferred to the transverse direction for instance. The comparison of macrographs in Fig. 16 shows flatter reinforcement and marginally shallower penetration for the sample achieved with the variable energy oscillation (Fig. 15d), but in any way, in both cases, good quality beads with low aspect of depth to width were achieved, which is not possible with a standard

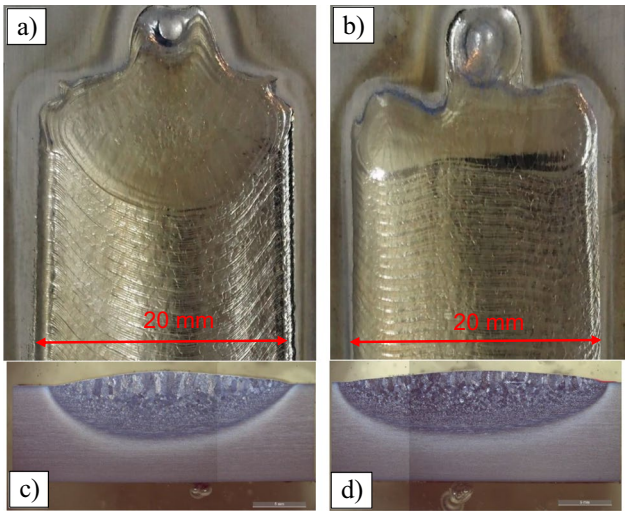

Fig. 15 Top beads and cross sections of bead appearances achieved by different oscillation strategies (Fig. 5) in dynamically controlled laser wire melting of Ti_6Al_4V; **a**, **c** fixed energy (constant scanning speed); **b**, **d** variable energy (variable scanning speed), travel speed 0.18 m/min, laser power 3 kW, laser spot size 4 mm with linear oscillation and amplitude 20 mm, wire feed rate 3 m/min

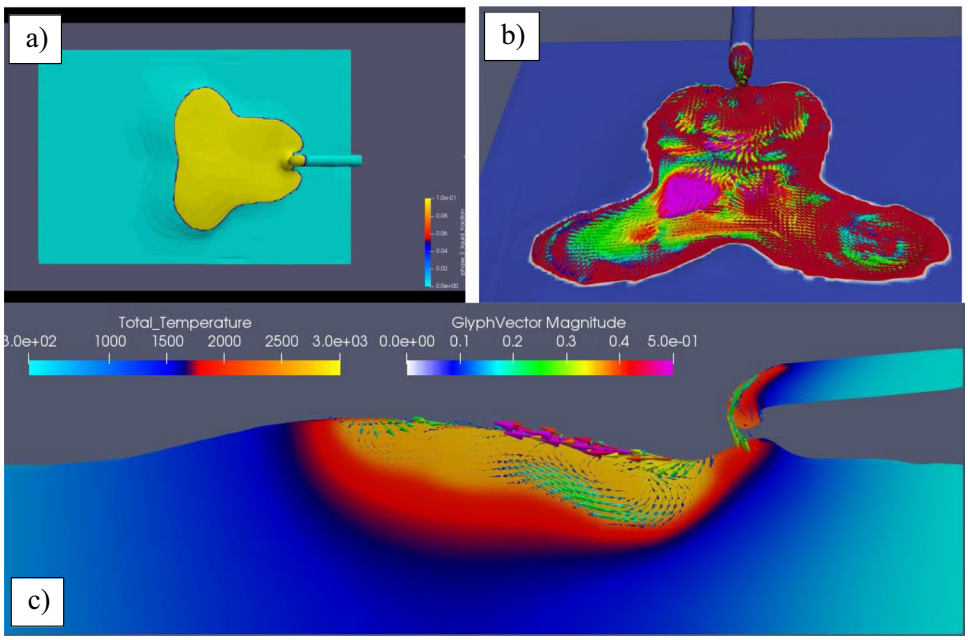

Fig. 14 Dynamically controlled laser wire melting of Ti_6Al_4V, travel speed 0.2 m/min, laser power 3 kW, laser spot size 4 mm with linear oscillation and amplitude 20 mm, wire feed rate 2 m/min; **a** combined energy profile, **b** top view of melt flow pattern, **c** longitudinal cross section indicating melt flow

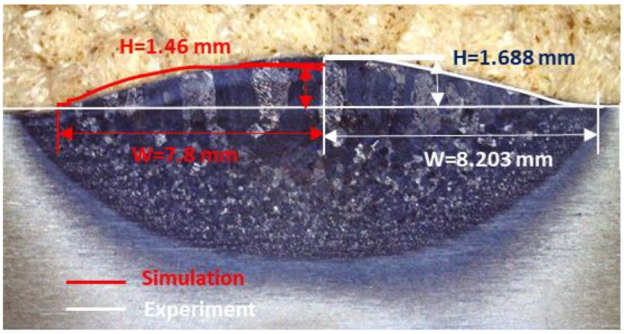

Fig. 16 Comparison of bead cross section between experiment and simulation in MES welding of Ti_6Al_4V, travel speed 0.18 m/min, laser power 1.2 kW, laser spot size 4 mm with linear oscillation and amplitude 12 mm, wire feed rate 3 m/min

laser beam profile. This demonstrates a great potential of advanced beam shaping in laser material processing applications. The results of experimental validation of the CFD modelling in Fig. 16 indicate good agreement.

The results show that through the smart application of laser energy, it is possible to tailor the melt flow and achieve stable melting regimes in laser processing. However, to be able to do this effectively, a good understanding of balancing forces is required, which can only be achieved by high fidelity numerical modelling.

4 Conclusions

Melt flow and bead shape development in several laser welding regimes was studied using CFD modelling and high-speed imaging. The following conclusions can be drawn from this research:

- In conduction laser welding or laser wire melting processes, the main flow is caused by the Marangoni convection, which can be controlled effectively by beam shaping.
- In the keyhole regime, the melt flow is more complex with several factors contributing to the net flow. Balancing all forces in the keyhole regime is more challenging with standard laser beams, which may lead to a narrow operating window for stable processing conditions. In this work, a new approach with concentric twin spots was demonstrated to stabilise the keyhole.
- Laser wobble welding requires optimum oscillation parameters for a given laser power and type of material. The process should be operated with optimum oscillation velocity for a given amplitude.
- A new concept of dynamic beam shaping has been developed and its ability to freely tailor the melt flow is demonstrated.

Funding The project was funded by an EPSRC Programme Grant Newam (EP/R027218/1).

Data Availability The data presented in this paper are available in Cranfield Research Information System (CRIS).

Declarations

Competing interests The authors declare no competing interests.

Open Access This article is licensed under a Creative Commons Attribution 4.0 International License, which permits use, sharing, adaptation, distribution and reproduction in any medium or format, as long as you give appropriate credit to the original author(s) and the source, provide a link to the Creative Commons licence, and indicate if changes were made. The images or other third party material in this article are included in the article's Creative Commons licence, unless indicated otherwise in a credit line to the material. If material is not included in the article's Creative Commons licence and your intended use is not permitted by statutory regulation or exceeds the permitted use, you will need to obtain permission directly from the copyright holder. To view a copy of this licence, visit http://creativecommons.org/licenses/by/4.0/.

References

1. Pang S, Chen L, Zhou J, Yin Y, Chen T (2011) A three-dimensional sharp interface model for self-consistent keyhole and weld pool dynamics in deep penetration laser welding. J Phys D Appl Phys 44:25301. https://doi.org/10.1088/0022-3727/44/2/025301
2. Tan W, Shin Y (2015) Multi-scale modeling of solidification and microstructure development in laser keyhole welding process for austenitic stainless steel. Comput Mater Sci 98:446–458. https://doi.org/10.1016/j.commatsci.2014.10.063
3. Dal M, Fabbro R (2016) [INVITED] An overview of the state of art in laser welding simulation. Opt Laser Technol 78:2–14. https://doi.org/10.1016/j.optlastec.2015.09.015
4. Liu G, Zhang Z, Wang H, Gui Y, Huang X, Li Y, Tan Y (2023) Influence of laser welding defocus and penetration monitoring based on advanced optical sensors. Optik (Stuttg) 280. https://doi.org/10.1016/j.ijleo.2023.170811
5. Rivera JS, Gagné M-O, Tu S, Barka N, Nadeau F, Ouafi AE (2023) Quality classification model with machine learning for porosity prediction in laser welding aluminum alloys. J Laser Appl 35. https://doi.org/10.2351/7.0000769
6. Laskin A, Laskin V (2011) Πshaper - refractive beam shaping optics for advanced laser technologies. J Phys: Conf Ser 276(12011):012171
7. Laskin A, Volpp J, Laskin V, Nara T, Jung SR (2021) Multispot optics for beam shaping of high-power single-mode and multimode lasers. J Laser Appl 33. https://doi.org/10.2351/7.0000461
8. Sundqvist J, Kaplan AFH, Shachaf L, Brodsky A, Kong C, Blackburn J, Assuncao E, Quintino L (2016) Numerical optimization approaches of single-pulse conduction laser welding by beam shape tailoring. Opt Lasers Eng 79:48–54. https://doi.org/10.1016/j.optlaseng.2015.12.001
9. Bourgin Y, Nagel F, Feßer P, Bergmann J-P, Sinzinger S (2018) High power laser beam shaping for welding applications by means of diffractive elements. In: Proceedings of the proceedings of SPIE - The International Society for Optical Engineering, vol 10744. Article number 107440X, Laser Beam Shaping XVIII 2018, San Diego

10. Möbus M, Woizeschke P (2023) Keyhole-in-keyhole formation by adding a coaxially superimposed single-mode laser beam in disk laser deep penetration welding. Weld World 67:1467–1478. https://doi.org/10.1007/s40194-023-01484-9
11. Papastathopoulos E, Baumann F, Bocksrocker O, Gottwald T, Killi A, Metzger B, Schad S-S, Speker N, Ryba T, Zaske S (2021) High-power high-brightness disk lasers for advanced applications. In: Proceedings of the proceedings of SPIE - The International Society for Optical Engineering, vol 116642021. Article number 116640M, Solid State Lasers XXX: Technology and Devices 2021, Virtual Online
12. Murzin SP, Kazanskiy NL, Stiglbrunner C (2021) Analysis of the advantages of laser processing of aerospace materials using diffractive optics. Metals (Basel) 11. https://doi.org/10.3390/met11060963
13. Kang M, Kim C (2020) Evaluation of hot cracking susceptibility on laser welded aluminum alloy using coaxially arranged multiple-beam laser. J Laser Appl 32. https://doi.org/10.2351/7.0000107
14. Lu Y, Deng Y, Shi L, Jiang L, Gao M (2023) Numerical simulation of thermal flow dynamics in oscillating laser welding of aluminum alloy. Opt Laser Technol 159:109003. https://doi.org/10.1016/j.optlastec.2022.109003
15. Song D, Kim R, Choi K, Shin D, Lee S (2023) Effects of beam shape on the microstructures and mechanical properties during thin-foil laser welding. Metals (Basel) 13. https://doi.org/10.3390/met13050916
16. Chelladurai Asirvatham M, Collins S, Masters I (2022) Laser wobble welding of steel to aluminium busbar joints for Li-ion battery packs. Opt Laser Technol 151. https://doi.org/10.1016/j.optlastec.2022.108000.
17. Kim K, Kang N, Kang M, Kim C (2022) Effect of laser beam wobbling on the overlap joint strength of hot-press-forming steel over 2.0 GPa tensile strength. J Laser Appl 34. https://doi.org/10.2351/7.0000447
18 Ki H, Mazumder J, Mohanty P (2002) Modeling of laser keyhole welding: Part I. mathematical modeling, numerical methodology, role of recoil pressure, multiple reflections, and free surface evolution. Metall Mater Trans A 33:1817–1830. https://doi.org/10.1007/s11661-002-0190-6
19. Le Masson P, Courtois M, Carin M, Gaied S, Balabane M (2014) A complete model of keyhole and melt pool dynamics to analyze instabilities and collapse during laser welding. J Laser Appl 26. https://doi.org/10.2351/1.4886835
20. Tan W, Shin YC (2014) Analysis of multi-phase interaction and its effects on keyhole dynamics with a multi-physics numerical model. J Phys D Appl Phys 47:345501. https://doi.org/10.1088/0022-3727/47/34/345501
21. Chen X, Zhou J, Shao X, Wang C (2015) 3D Transient multiphase model for keyhole, vapor plume, and weld pool dynamics in laser welding including the ambient pressure effect. Opt Lasers Eng 74. https://doi.org/10.1016/j.optlaseng.2015.05.003
22. Hirt CW, Nichols BD (1981) Volume of Fluid (VOF) Method for the dynamics of free boundaries. J Comput Phys 39:201–225. https://doi.org/10.1016/0021-9991(81)90145-5
23. Bombardelli F, Meireles I, Matos J (2010) Laboratory measurements and multi-block numerical simulations of the mean flow and turbulence in the non-aerated skimming flow region of steep stepped spillways. Environ Fluid Mech 11:263–288. https://doi.org/10.1007/s10652-010-9188-6
24. Voller VR, Brent AD, Prakash C (1989) The modelling of heat, mass and solute transport in solidification systems. Int J Heat Mass Transf 32:1719–1731. https://doi.org/10.1016/0017-9310(89)90054-9
25. Chen X, Wang C, Ding J, Bridgeman P, Williams S (2022) A three-dimensional wire-feeding model for heat and metal transfer, fluid flow, and bead shape in wire plasma arc additive manufacturing. J Manuf Process 83:300–312. https://doi.org/10.1016/j.jmapro.2022.09.012
26. Hu R, Chen X, Yang G, Gong S (2018) Metal transfer in wire feeding-based electron beam 3D printing: modes, dynamics, and transition criterion. Int J Heat Mass Transf 126. https://doi.org/10.1016/j.ijheatmasstransfer.2018.06.033
27. Chen X, Wang C, Ding J, Qu R, Wang Y, Pardal G, Williams S (2023) Thermal Fluid Dynamics of the effect of filler wire on deposition rate and bead formation intending plasma arc-based DED. J Manuf Process 107:199–209. https://doi.org/10.1016/j.jmapro.2023.10.020
28. Katayama S (2013) Defect formation mechanisms and preventive procedures in laser welding. In: Handbook of laser welding technologies, pp 332–373
29. Chen G, Williams S, Ding J, Wang C, Suder W (2022) Multi-energy source (MES) configuration for bead shape control in wire-based directed energy deposition (w-DED). J Mater Process Technol 304. https://doi.org/10.1016/j.jmatprotec.2022.117549

Publisher's Note Springer Nature remains neutral with regard to jurisdictional claims in published maps and institutional affiliations.

https://dspace.org/

Control of meltpool shape in laser welding

Suder, Wojciech; Chen, Xin; Rico Sierra, David; Chen, Guangyu; Wainwright, James ...

2024-03-05
Springer
https://doi.org/10.1007/s40194-024-01719-3
Suder W, Chen X, Sierra DR, et al., (2024) Control of meltpool shape in laser welding. Welding in the World, Volume 68, June 2024, pp. 1485-1495

Downloaded from a DSpace repository. https://dspace.org/